Solution Properties of Star and Linear Poly(*N*-isopropylacrylamide)

Ronda Plummer, David J. T. Hill, and Andrew K. Whittaker*

Australian Institute for Bioengineering and Nanotechnology, and Centre for Magnetic Resonance, University of Queensland, QLD 4072, Australia

Received June 28, 2006; Revised Manuscript Received September 20, 2006

ABSTRACT: The LCST transitions of novel *N*-isopropylacrylamide (NIPAM) star polymers, prepared using the four-armed RAFT agent pentaerythritoltetrakis(3-(*S*-benzyltrithiocarbonyl)propionate) (PTBTP) and their hydrolyzed linear arms were studied using ^{1}H NMR, PFG-NMR, and DLS. The aim was to determine the effect of polymer architecture and the presence of end groups derived from RAFT agents on the LCST. The LCST transitions of star PNIPAM were significantly depressed by the presence of the hydrophobic star core and possibly the benzyl end groups. The effect was molecular weight dependent and diminished once the number of repeating units per arm ≥70. The linear PNIPAM exhibited an LCST of 35 °C, regardless of molecular weight; the presence of both hydrophilic and hydrophobic end groups after hydrolysis from the star core was suggested to cancel effects on the LCST. A significant decrease in R_H was observed below the LCST for star and linear PNIPAM and was attributed to the formation of *n*-clusters. Application of a scaling law to the linear PNIPAM data indicated the cluster size $n = 6$. Tethering to the hydrophobic star core appeared to inhibit *n*-cluster formation in the lowest molecular weight stars; this may be due to enhanced stretching of the polymer chains, or the presence of larger numbers of *n*-clusters at temperatures below those measured.

Introduction

Aqueous solutions of poly(*N*-isopropylacrylamide) (PNIPAM) exhibit a lower critical solution temperature (LCST) transition at 32 °C; above this temperature, the solubility of the polymer is vastly reduced.[1] The LCST is considered to be due to a balance of hydrogen bonding and hydrophobic interactions influencing polymer−solvent and polymer−polymer interactions.[1] The LCST behavior of aqueous PNIPAM solutions has been widely studied; the presence of comonomers, cross-linking, grafting, end groups, and the addition of cosolutes all affect the phase transition of PNIPAM.[1−5] The thermoresponsive behavior of PNIPAM has applications in fields such as surface modification[6] and drug delivery.[7−9] Research in polymer physics aims to provide deeper understanding of the LCST phenomenon and the factors influencing it.[10−12] The LCST transition can be studied using a variety of analytical methods including ^{1}H NMR,[13] PFG-NMR,[14] dynamic light scattering (DLS),[15,16] fluorescence,[17] differential scanning calorimetry,[18] and cloud point determination using UV−vis spectrophotometry.[1,3]

Many earlier studies employed PNIPAM prepared using traditional free radical polymerization, and therefore, the polymers were highly polydisperse. High polydispersity is undesirable because the LCST has been reported to be chain length dependent[18,19] in some cases, and independent of chain length in others,[20] so the varying results may be influenced by polydispersity. The advent of living polymerization, especially RAFT, has allowed the synthesis of linear PNIPAM of low polydispersity.[3,9,16,21] However, a factor to be considered is that end groups will be present from initiators or RAFT agents with living polymerization methods and will either depress or elevate the LCST depending on their nature. A number of studies have focused on the influence of hydrophobic and hydrophilic end groups or copolymers on the LCST behavior of linear PNIPAM, and generally, hydrophobic groups tend to lower the LCST by promoting polymer−polymer interactions and hydrophilic groups tend to increase it by promoting polymer−solvent interactions.[1,8,9,21,22] The influence is generally molecular weight dependent and diminishes with increasing chain length. Schilli et al. have studied the effect of RAFT agent end groups on the LCST of linear PNIPAM.[9] The RAFT agent used was benzyl 1-pyrrolecarbodithioate, so one end of the chain contained a benzyl group and the other a pyrrole dithioester group. They found the LCST decreased almost linearly with increasing reciprocal molecular weight. The cloud point of the linear PNIPAM used in their study approached 32 °C at a molecular weight of ≥20 000 g/mol. A similar trend was observed by Xia et al. for linear PNIPAM containing groups of varying hydrophobicity prepared using ATRP.[21] To date, however, the behavior of PNIPAM star polymers has not been investigated.

The behavior of PNIPAM chains grafted to surfaces has also been intensively studied. The effect of tethering a PNIPAM chain to a surface (planar or spherical) is to change the phase transition behavior in subtle ways, depending on the curvature of the surface and grafting density.[10,14,23−26] The study of polymer chains tethered at one end to a curved surface includes systems such as chains grafted to small colloidal particles, the corona of polymeric micelles, and the arms of star and comb polymers.[27] A number of theoretical models and simulations have been developed to explain the changed behavior of grafted chains compared with free chains in solution.[11,27−29]

A study of the combined influence of tethering PNIPAM chains to the star RAFT agent core (Z group), and the presence of the end group (R group) on LCST behavior of PNIPAM stars is of interest for a number of reasons. The effect of tethering PNIPAM to the star core is expected to produce a similar effect to grafting to a spherical surface of minimum radius;[30] the LCST behavior may therefore be expected to change, and it may be possible to explain the changed behavior using an existing model.[11,23,24,28] Previous studies of the influence of a hydrophobic end group indicate that a lowering of the transition is to be expected as a result of increased hydrophobic interactions.[8,9] Determination of the LCST of the liberated arms of the star polymers would then provide evidence as to whether the core

* Corresponding author. Email: andrew.whittaker@cmr.uq.edu.au. Telephone: +61 7 3365 4100. Fax: +61 7 3365 3833.

10.1021/ma0614545 CCC: $33.50
Published on Web 10/31/2006

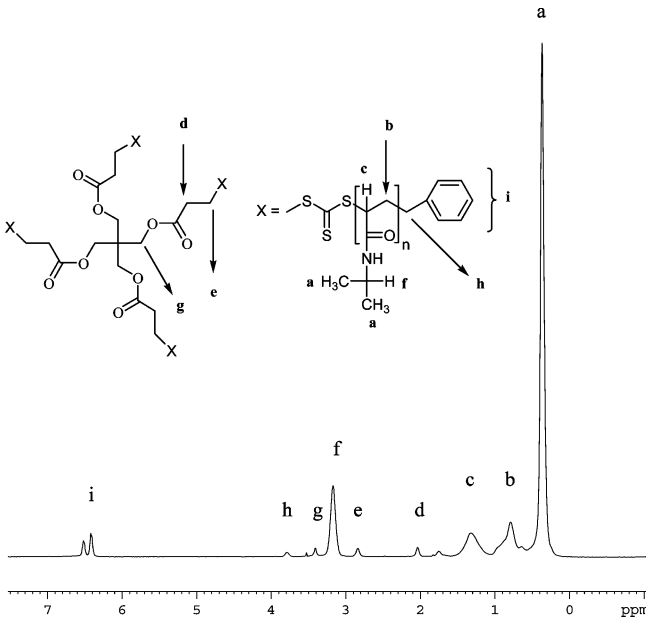

Figure 1. PFG-NMR ^{1}H spectrum of 10k target PNIPAM star prepared by RAFT polymerization in DMF at 60 °C using PTBTP; PNIPAM signals and RAFT agent signals are labeled; solvent signals have been diffusion edited for clarity.

or the end group has most influence. It would be useful to know the molecular weight at which these two influences cease to affect the LCST so that polymers could be tailored for specific applications. Figure 1 shows the structure of the PNIPAM star used for this work and the linear chain after cleavage from the trithiocarbonate core.

In this paper, the aqueous solution behavior of a range of novel PNIPAM star and linear polymers were studied using proton NMR and dynamic light scattering (DLS). ^{1}H spectra, pulsed field gradient NMR (PFG-NMR), and DLS measurements were used to characterize the LCST via changes in integrated NMR peak areas and hydrodynamic radii of the polymers. The effects of the star architecture on the transition temperature of PNIPAM as a function of molecular weight and comparison with the LCST behavior of the liberated arms of the star polymer after nucleophilic cleavage of the trithiocarbonate linkage were investigated.

Experimental Section

Materials. All synthetic reagents were analytical grade or higher and used as received unless stated otherwise. *N*-isopropylacrylamide (NIPAM) (Aldrich, 97%) was recrystallized from toluene/hexane 3:2 and dried in vacuo before use. PNIPAM star polymers were prepared by reversible addition−fragmentation chain transfer (RAFT) polymerization in *N*,*N*-dimethylformamide (DMF) using the four-armed RAFT agent pentaerythritoltetrakis(3-(*S*-benzyltrithiocarbonyl)propionate) (PTBTP). The synthesis of PTBTP has been reported in the literature.[31]

Polymerizations. For example, to prepare a target molecular weight of 10 000 at 80% conversion, a stock solution of NIPAM (4 M), azobis(isobutyronitrile) (AIBN) (5.33×10^{-3} M), and PTBTP (4×10^{-2} M) in DMF was prepared. Generally, 0.5 mL aliquots of the stock solution were transferred to 2 mL tubes and deoxygenated by four freeze−evacuate−thaw cycles and flame-sealed under vacuum. Polymerization was conducted at 60 °C in a constant temperature water bath, and samples removed at regular intervals to determine conversion using FT-NIR. Dried PNIPAM was dissolved in acetone and then precipitated by addition to an excess of hexane; this method provided polymers of acceptable purity as determined by ^{1}H NMR.

Cleavage of NIPAM Star Polymer Arms with Piperidine. Star polymers (10−20 mg) were dissolved in DMF (1 mL) and treated with piperidine (100 μL). Monitoring the reaction using GPC revealed that the reaction was complete for PNIPAM stars within 1 h. The linear PNIPAM was purified by dissolving in acetone and precipitating into an excess of hexane. The linear NIPAM chains used in this study thus refer to the hydrolyzed arms of the corresponding star polymer.

Polymers were dissolved at a concentration of 1 or 10 mg/mL in D_2O, and equilibrated for up to 1 week before measurement. Polymer solutions were stored in a refrigerator at 3−5 °C. A 1[7,32] or 10 mg/mL[2,14] concentration is commonly used for NMR and cloud point studies of PNIPAM. The polymer solutions studied had pH = 8 because this was the pH of the D_2O used.

PFG-NMR Diffusion Measurements. NMR spectroscopy was carried out using a Bruker Avance DRX 500 spectrometer operating at 500.13 MHz for protons and equipped with a 5 mm triple resonance (^{1}H, ^{13}C, ^{15}N) *z*-gradient probe equipped with actively shielded gradients. The *z*-gradient was calibrated at 298 K with a HDO sample containing 0.1 mg mL^{-1} $GdCl_3$. The maximum *z*-gradient amplitude was 5 T/m. A bipolar pulse longitudinal eddy current delay (BPPLED)[33] pulse sequence, or if convection was a problem, a bipolar pulse pair double stimulated echo pulse sequence (BPPDSTE)[34] pulse sequence was used. The pulse sequences included a 5 ms delay to allow residual eddy currents to decay. Sine-shaped gradient pulses were utilized to further minimize eddy currents. The pulse gradient duration δ, was chosen for each diffusion time in order to obtain the minimum residual signal for each component at maximum gradient strength. The pulse gradients were incremented from 2 to 95% of the maximum gradient strength in a linear ramp (24 steps). A spectral window of 6000 Hz was accumulated in an acquisition time of 2.7 s. A relaxation delay of $5 \times T_1$ of the slowest relaxing signal was used (10 s). The free induction decays were collected into 16k data points; 16−32 scans and 4 dummy scans were acquired on each sample. Following acquisition, the free induction decays were Fourier transformed by applying zero-filling to 32k data points and an exponential window function with a line broadening factor of 1−5 Hz.

Data were processed using Bruker XWINNMR software; the diffusion coefficients were obtained from a single- or double-exponential nonlinear least-squares fitting of the peak intensities. The diffusion coefficients for PNIPAM samples were obtained from a single-exponential fit of the echo attenuation decay of the methyl protons of the isopropyl side chain because this signal had the best signal-to-noise ratio. Diffusion coefficients were obtained by monitoring the signal attenuation as a function of the applied magnetic field gradient amplitude (g) and fitting eq 1 to the results.[35]

$$I = I_0 \exp\left(-D\gamma^2\delta^2 g^2(\Delta - \delta/3)\right) \quad (1)$$

where I is the resonance intensity measured for a given gradient amplitude, g, I_0 is the signal intensity with no gradient applied, γ is the gyromagnetic ratio, δ is the gradient length, and Δ is the diffusion time.

Dynamic Light Scattering. Dynamic light scattering analysis was performed on a Malvern Zetasizer Nano ZS system equipped with a single angle 173° backscatter system incorporating a He−Ne laser (λ = 633 nm). A Peltier controller was used to adjust the temperature. Polymers were dissolved at a

Table 1. M_n and PDI Data for PNIPAM Star Polymers, and Linear Polymers Obtained by Hydrolysis of the CTA Trithiocarbonate Core

star MW (NMR)	repeating units/arm	PDI (GPC)	linear chain MW (NMR)	repeating units	PDI (GPC)
10 200	20	1.18	3206	28	1.09
13 117	26	1.22	8500	74	1.04
32 800	70	1.26	11700	102	1.1
52 680	114	1.27			

concentration of 0.25 and 1 mg/mL in D_2O, and equilibrated for up to 1 week before measurement. Samples for DLS experiments were filtered through 0.45 μm PTFE filters prior to measurement and equilibrated for 20 min at each change in temperature. The DLS particle diameters were calculated using the Stokes−Einstein equation using the viscosity values for D_2O obtained from the literature. The volume distribution results were used for all samples. Data were processed using Malvern DTS software version 4.00.

LCST Determination. Proton NMR measurements: the methyl protons of PNIPAM were chosen for peak area integration in each experiment because this peak had the best signal-to-noise ratio. The peak area at each temperature was normalized relative to the peak area of the lowest temperature experiment for that polymer (determined to be below the LCST). Samples were equilibrated at each temperature for 30 min prior to NMR measurements. The LCST was defined as the temperature corresponding to a reduction in integrated NMR peak area of 50%. The criteria for identifying the LCST varies; some authors state the onset of turbidity as the LCST,[7] others define the inflection point in the cloud point curve as the LCST,[32] or 50% reduction in transmittance.[8] In the current work, the point at which the peak area decreased by 50% was the easiest to identify and thus considered the most accurate. For DLS measurements, the LCST was identified by a sudden change in particle size.

Gel Permeation Chromatography. Polymer molecular weight and polydispersity data were obtained using a Waters Alliance 2690 separations module equipped with an autosampler, column heater, differential refractive index detector, and UV−visible detector. *N*,*N*-Dimethylacetamide (DMAC) containing 0.03 wt % LiCl was used as eluent at a flow rate of 1 mL min^{-1}. Two Styragel columns (3 HT and 6E HT: 500−30 000, and 5000−1 × 10^7 effective molecular weight range respectively) maintained at 70 °C were used for separation. Polystyrene standards ranging from 500 to 2^6 g mol^{-1} were used for calibration. Polymers were not purified prior to GPC analysis. Standard and sample solutions were prepared at 2 mg mL^{-1} concentration and filtered through a 0.45 μm PTFE filter. Data were processed with Millenium[32] software. Molecular weights are reported relative to poly(styrene).

Results and Discussion

Effect of Molecular Weight and Molecular Architecture on the LCST of PNIPAM. Table 1 lists the values of molecular weight and polydispersity of the star and linear PNIPAM used in the following experiments. Polymers were dissolved at a concentration of 1 or 10 mg/mL in D_2O and equilibrated for up to 1 week before measurement. NMR experiments provide dynamic information about the local segmental mobility of a polymer chain. Solution NMR selectively detects only liquid spins; "solid" spins are not detected because their restricted mobility produces extremely broad signals due to dramatically shortened T_2 relaxation times.[14] The mobility of polymer chains as a function of temperature or concentration can therefore be studied.

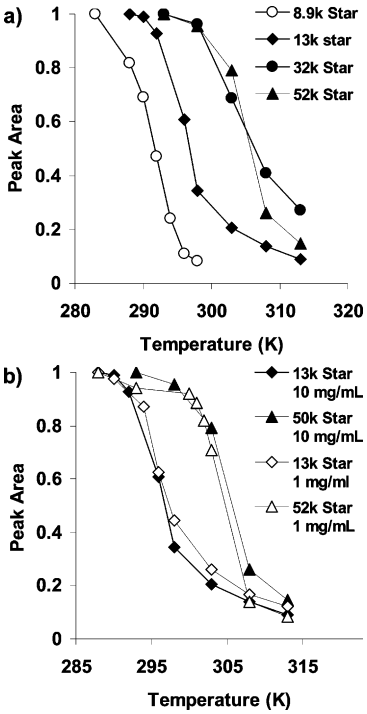

Figure 2. Integrated methyl proton peak area as a function of temperature obtained from ^1H NMR for (a) 10k, 13k, 32k, and 52k PNIPAM star polymers = 10 mg/mL in D_2O; (b) comparison of 10 and 1 mg/mL data for 13k and 52k PNIPAM stars in D_2O.

The integrated peak areas of the methyl protons of the PNIPAM stars as a function of temperature are displayed in Figure 2. The methyl proton peak areas decreased with increasing temperature; all other PNIPAM signals showed a very similar reduction in peak intensity with increasing temperature. The decrease in the peak area as a function of temperature reflects the number of mobile polymer segments and can therefore distinguish the phase transition. Significantly, the aromatic signals of the RAFT agent benzyl group, situated on the ends of the PNIPAM chains, exhibited a similar reduction in peak intensity to the PNIPAM signals with increasing temperature. This suggests that the benzyl group is interacting with the PNIPAM and is affected by the polymer phase transition (discussed below). The PNIPAM samples in this study did not exhibit peak broadening as a result of chain immobilization with increasing temperature. The ^1H NMR spectra at each temperature were almost identical; T_2 relaxation times were measured on selected samples and showed minimal variation with increasing temperature through the LCST transition, indicating that a range of spin environments of differing mobility were not present. In this case, the spins either maintained mobility or became "solid". Peak broadening has been observed along with shorter T_2 relaxation times in NMR studies of the LCST of PNIPAM and other polymers which exhibit an LCST.[13,36]

All polymer solutions were turbid above the measured LCST and eventually precipitated completely over a 12−24 h period. This behavior reflects an initial intramolecular chain collapse, followed by slow interchain aggregation.[1,15,37] No hysteresis was observed for the PNIPAM samples in this work; the PNIPAM solutions redissolved completely upon cooling below the LCST.

The phase transition temperature of the star polymers increased with increasing molecular weight; for the 10k PNIPAM star, the LCST was approximately 290 K, the 13k star showed a transition around 296 K, and for the 32k and 52k polymers, the transitions were in the range 305−306 K. The

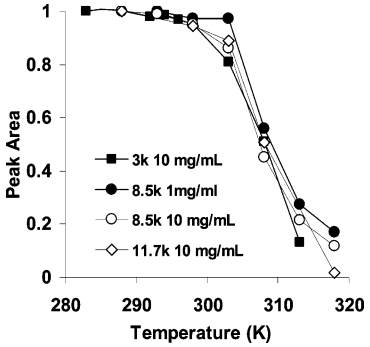

Figure 3. Change in peak area with temperature for PNIPAM linear polymers; 3k, 8.5k, and 11.7k at 10 mg/mL concentration in D_2O, 8.5k linear PNIPAM at 1 mg/mL concentration in D_2O.

LCST observed for the 32k and 52k PNIPAM stars was close to the literature value of 305 K (32 °C) reported for high-molecular-weight linear PNIPAM.[1] It appears that, once a certain number of repeating units are present (in this case ≥70), there is no depression of the LCST. The LCSTs observed for the 10k and 13k polymers are 15 and 9 degrees lower, respectively, than for linear PNIPAM. The depression of the LCST observed for the lower-molecular-weight stars indicates that either the effect of anchoring to the hydrophobic RAFT agent star core (Z group) and/or the presence of the benzyl end group originating from the RAFT agent R group is enhancing hydrophobic interactions; increasing hydrophobicity is known to lower the LCST of PNIPAM.[1,8,9,21,22] Each arm consists of approximately 20 and 26 NIPAM repeating units for the 10k and 13k stars, respectively, so the influence of the core/end group should be more significant for these smaller polymers than for the higher-molecular-weight star polymers. The data in Figure 2b demonstrates that polymer solution concentration has little influence on the LCST behavior of the PNIPAM stars, at least in the range studied; similar transition behavior was observed for 10 and 1 mg/mL concentrations, indicating minimal chain entanglement occurred below the LCST at these concentrations.

To clarify the influence of the RAFT agent core and end group on the LCST of the PNIPAM stars, the arms of the stars were cleaved at the trithiocarbonate linkage using piperidine as described in the Experimental Section. The completeness of the reaction was checked using GPC, the polymers were purified by precipitation, and the NMR experiments repeated under identical conditions and concentrations.

PNIPAM chains liberated from the core of the 13k, 32k, and 52k molecular weight star polymers were found by ^{1}H NMR end group analysis to have molecular weights of 3200, 8500, and 11 700 (Table 1). The integrated peak areas of the methyl protons of the linear PNIPAM as a function of temperature are displayed in Figure 3. Surprisingly, all linear PNIPAM chains exhibited an LCST of 307−308 K (34−35 °C). Comparison of the LCST values obtained for the star and linear PNIPAM suggest that attachment to the RAFT agent star core was the cause of the depressed LCST observed for the 10k and 13k star polymers. This may reflect either the increased overall hydrophobicity of the smaller polymers due to the combined influence of the RAFT agent core and benzyl end group, a chain-length-dependent effect of tethering to the RAFT agent core, or a combination of these effects. The influence of tethering to the central core is thus molecular weight dependent and disappears once the number of repeating units is ≥70. The LCST values for the 32k and 52k PNIPAM stars are lower than those of the linear PNIPAM chains; this may suggest a small effect of tethering the chains to the star core, or the linear PNIPAM LCST may be elevated for some reason.

The LCST of 307−308 K obtained for the linear PNIPAM is higher than the 305 K usually observed for linear PNIPAM of larger molecular weight,[1] but this is not surprising. The LCST observed for low-molecular-weight linear PNIPAM chains has been shown to increase with decreasing molecular weight; the transition temperature is expected to decrease with increasing molecular weight as a result of the smaller combinatorial entropy with increasing chain length.[12]

The results obtained for the linear PNIPAM indicate that the benzyl end group is having a negligible effect on the LCST, suggesting that only the core (or combination of the core *and* benzyl group) results in depression of the LCST. This is an unusual outcome considering many previous studies on the effects of hydrophobic end groups and substituents on the LCST of PNIPAM. In general, as the ratio of PNIPAM to hydrophobic end group decreases, the LCST is expected to decrease; the decrease should be especially significant for the smallest 3k PNIPAM chains, but no effect is apparent.

One possible explanation for the LCST behavior of the linear PNIPAM could be the formation of micelles with the benzyl groups as the core and PNIPAM as the corona. Micelle formation has been observed in a number of studies using linear PNIPAM with hydrophobic end groups.[5,8,14,16] Winnik et al. studied PNIPAM containing two pendant *n*-octadecyl groups on the chain end.[5] They observed an LCST for the polymer very close to 32 °C, and demonstrated using dynamic light scattering that micelle formation occurred at concentrations exceeding 0.1 mg/mL. The alkyl chains were isolated from the solvent in the micelle core and so did not make the expected hydrophobic contribution to the LCST. The PNIPAM chains formed the corona and exhibited an LCST in the normal range. A micelle consisting of a hydrophobic core of benzyl groups and a PNIPAM corona is possible in the present case, but the experimental data suggests otherwise. Benzyl groups aggregated in the interior of a micelle would experience low solvation and restricted molecular motion; a reduction (or even disappearance) of the aromatic signal intensity[38] due to low solvation and a shortened T_2 relaxation time would then be expected compared with the corresponding star, and this was not observed (within experimental error). In addition, aromatic groups exhibit both a reduced hydrophobicity and larger rigidity compared with alkyl chains; these attributes tend to hinder self-assembly in water.[39] If a micelle did form and the aromatic core was sufficiently well-solvated and mobile enough to prevent loss of NMR signal intensity, a suppression of the LCST would be expected for the 3k chains, but this was not observed.

Another possible explanation for the observed LCST behavior of the linear PNIPAM is the presence of a hydrophilic group on the opposite end of the PNIPAM chain. A thiol is expected to form during the cleavage reaction with piperidine,[40] but would not be detected in the ^{1}H NMR spectrum because of chemical exchange with deuterium. In any case, the presence of a relatively hydrophilic group such as a thiol on the opposite end of the polymer chain may offset the hydrophobic effect of the benzyl group. Hydrophilic end groups generally result in an increase in the LCST,[1] so the overall effect would be to cancel the end group influence on the transition. Such a scenario could produce the LCST behavior observed for the linear PNIPAM.

There are numerous reports that show either no influence of end groups on LCST as a function of molecular weight, or a strong influence. For example, linear PNIPAM containing a terminal carboxyl group via chain transfer polymerization with

3-mercaptopropionic acid had an identical LCST transition to nonfunctionalized PNIPAM for molecular weight 1300−19 000.[41,42] Conversely, Xia et al.[21] recently reported a 5.4 °C decrease in LCST with an increase in molecular weight from 3000 to 7300 for linear PNIPAM containing ethyl 2-chloropropionate end groups. On the basis of the above discussion, the effect of the benzyl end group on the LCST transitions observed for the linear and star PNIPAM cannot be predicted. Diffusion and dynamic light scattering studies (discussed below) were conducted in order to clarify whether end group effects or micelle formation were responsible for the elevated LCST of the linear PNIPAM.

There was a linear dependence of LCST on the reciprocal M_n for the PNIPAM star polymers (data not shown). A similar dependence of LCST on M_n was observed by Schilli et al. for linear PNIPAM prepared by RAFT polymerization.[9] The linear PNIPAM in this work did not exhibit any dependence of LCST on chain length in the molecular weight range 3−11.7k; the presence of the thiol end groups may explain this observation as discussed above.

Width of the LCST Transition of Star and Linear PNIPAM. The transitions observed for all PNIPAM in the current study using NMR are less well defined than the sharp 1−2 °C transition commonly observed for linear PNIPAM using cloud point, ^{1}H NMR, or DLS.[1,14] The transitions occur over a range of approximately 10−15 °C (Figures 2 and 3). This is unexpected for polymers of low PDI. Zhulina et al.[10] have predicted transition broadening on theoretical grounds for chains attached to surfaces compared with an isolated three-dimensional chain. The effect was ascribed to interchain interactions within layers for chains attached to a surface producing a weaker phase transition, the effect becoming more pronounced with a decrease in the dimensionality of the chains in the layer and with increased grafting density. The broad transition is present for all PNIPAM samples in the present study, so unless the linear PNIPAM does form a micelle, and formation of a micelle produces an effect similar to tethering, this does not explain the increased transition width in this case.

The broadening of the phase transitions observed for both star and linear PNIPAM suggests that the origin of the broadening is not a function of molecular weight, at least not within the molecular weight ranges studied, and not due to the tethering of the PNIPAM chains to the star core. It has been demonstrated that an increase in the degree of polymerization tends to sharpen the LCST.[43,12] Schild et al.[18] have observed that linear PNIPAM of high polydispersity (2.3−6.9) exhibited a broadened phase transition; this reflects the contributions from a variety of chain lengths. The molecular weights of PNIPAM used for this work are low relative to the molecular weight of linear PNIPAM used in most studies (usually >100k), so it seems plausible that the low molecular weight of these chains results in the observed transition broadening. The broadening was not a function of concentration over a 10-fold change in polymer solution concentration, and the concentrations used were below the overlap concentration as determined from PFG-NMR diffusion measurements (discussed below).

Pulsed Field Gradient NMR Studies of the Hydrodynamic Behavior of Star and Linear PNIPAM over the LCST Transition. PFG-NMR was used to measure diffusion coefficients of the star and linear PNIPAM as a function of temperature. The samples used for diffusion experiments were the same as those used for the ^{1}H NMR experiments described above (1 and 10 mg/mL in D_2O). Diffusion coefficients were normalized for temperature and viscosity using viscosity values for D_2O at various temperatures obtained from the literature. Once the diffusion coefficients were known, estimation of the hydrodynamic radii of the polymers as a function of temperature was possible using the Stokes−Einstein equation:

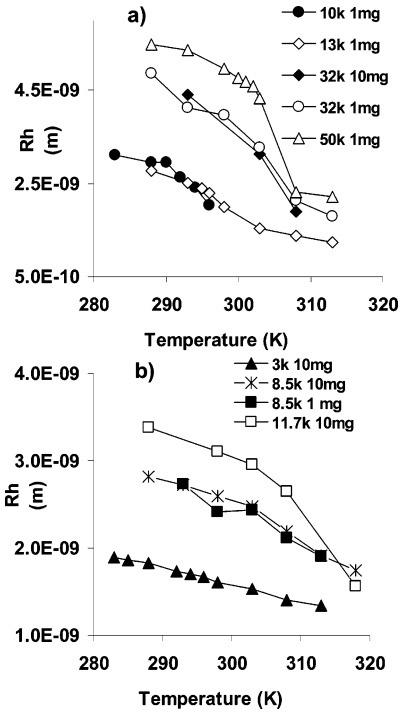

Figure 4. Hydrodynamic radii of star and linear PNIPAM as a function of temperature; (a) 10k, 13k, 32k, and 52k PNIPAM star polymers: 1 mg/mL in D_2O, and 32k PNIPAM star 10 mg/mL in D_2O; (b) 3k, 8.5k, and 11.7k linear PNIPAM 10 mg/mL, and 8.5k linear PNIPAM 1 mg/mL in D_2O.

$$D = kT/(6\pi\eta R_H) \quad (2)$$

Here k is the Boltzmann constant, T is the temperature, η is solution viscosity, and R_H is the hydrodynamic radius (for the simple case of a spherical particle).[35]

Figure 4 shows the hydrodynamic radii for the star and linear PNIPAM as a function of temperature. A steady decrease in R_H is observed with increasing temperature for all samples *below* the LCST and occurs over a broad range of temperatures. The significant decrease in R_H below the LCST suggests a considerable change in the PNIPAM chain conformation occurs below the phase transition. A more dramatic decrease in R_H occurs around the phase transition as expected because chain collapse results in a more compact particle. The 3k linear polymer shows a steady decline in R_H across the transition with no dramatic change occurring at the LCST, but in general, all the PNIPAM samples show a relatively steady decline in R_H across the transition. The highest-molecular-weight star and linear PNIPAM show a somewhat sharper transition, however. These observations suggest that the transition is not discontinuous (of first order), but continuous and of second order.[24,44] This may be a function of the small number of repeating units because increasing chain length has been shown to sharpen the LCST.[43,44] Concentration effects were not observed between 1 and 10 mg/mL for either the star or linear PNIPAM, as shown in Figure 4a−b for the 32k star and 8.5k linear samples, respectively.

Information on the conformation of the PNIPAM chains in a good solvent may be obtained by comparing the root-mean-square (rms) end-to-end distance for free PNIPAM chains in solution to the R_H values obtained experimentally via PFG-

Table 2. R_H and rms End-to-End Distances Calculated for Star and Linear PNIPAM at 288 K

MW (NMR)	R_H (nm) (NMR)	diameter (nm) (NMR)	calculated RMS end-to-end distance (nm)	measured diameter as % rms size
		Star		
10 200	2.92	5.84	10.71	54.5
13 117	2.78	5.56	12.11	45.9
32 800	4.87	9.74	18.79	51.8
52 680	5.49	10.98	23.69	46.3
		Linear		
3 206	1.83	3.66	5.9	62
8 500	2.82	5.64	9.5	59.4
11 700	3.38	6.76	11.13	61

NMR. The rms end-to-end distance was calculated using the relation:[24]

$$(r^2)^{1/2} = C_\infty^{1/2} l n^{1/2} \quad (3)$$

where C_∞ is the characteristic ratio of PNIPAM $= 25 \pm 1$,[24] l is the C−C bond length, and n is number of backbone bonds (including the star RAFT agent core). The measured R_H values and calculated rms end-to-end distances for the star and linear PNIPAM are shown in Table 2. The R_H values shown were those obtained at 288 K, i.e., well below the LCST, and therefore apply for the polymer in a good solvent. The R_H values were converted into diameters and compared with the calculated rms end-to-end distance values; the diameters are approximately 50% and 60% of the calculated chain dimensions for the star and linear polymers, respectively. While some uncertainty in the NMR measurement and from the use of the Stokes−Einstein equation for a hard sphere is expected, the measured radii indicate that the star and linear PNIPAM form relatively compact structures in solution in a good solvent and that the linear polymers are slightly more expanded than the stars.

As mentioned above, the aromatic signals of the RAFT agent benzyl group showed a similar reduction in NMR peak area intensity as the PNIPAM, suggesting that the benzyl group, situated on the end of the PNIPAM chain (see Figure 1), was interacting with the PNIPAM. It is likely that the end groups become trapped by the collapsing PNIPAM chains at the LCST, reducing the mobility of the aromatic protons and causing a reduction in signal intensity. The compact size of the linear and star PNIPAM may reflect this interaction; the polymer may adopt a conformation where the chain ends are enclosed by the PNIPAM chains. In the case of the star polymers, an association between the benzyl groups and the hydrophobic RAFT agent core is also possible.

The 10k PNIPAM star has a larger R_H than that of the 13k star; this may be due to experimental error or may indicate that the 10k star arms are more stretched because tethering causes chains to stretch in a direction perpendicular to the interface due to strong interarm repulsions in the core.[27,45,46] The expansion or extension of the polymer chains in the core region can extent over most of the length of the polymer having small molecular weight and reduces in importance with increasing molecular weight.[45]

It is apparent from the data in Table 2 that the R_H values for the linear chains are less than those obtained for the parent stars, verifying that the linear PNIPAM does not form micelles at 288 K. This trend occurs throughout the temperature range as depicted in Figure 4; no increase in R_H due to the formation of larger (NMR observable) particles is apparent. At 288 K, D_2O is a good solvent for PNIPAM, and as the temperature increases, the solvent quality becomes poorer. A portion of the NMR signal is therefore becoming NMR invisible (due to a shorter T_2) as the temperature increases (see Figures 2 and 3). If aggregates form between the linear chains, these may not be NMR visible and may explain why no evidence of a slow-diffusing component was observed in the diffusion decay curves.

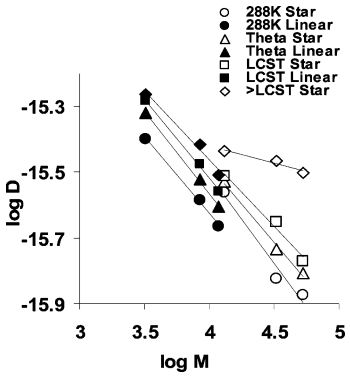

Figure 5. Molecular weight dependence of the diffusion coefficient for star and linear PNIPAM over a range of temperatures. Lines are the least-squares fits to the data.

For a comparison of hydrodynamic properties of star and linear PNIPAM of similar molecular weight, the 10k and 13k stars can be compared to the 11.7k linear PNIPAM. The R_H for the 10k and 13k stars were 2.92 and 2.78 nm, respectively; the 11.7k linear PNIPAM R_H was 3.38 nm. These results are in agreement with theoretical predictions; branching results in a contraction relative to the linear chain of similar molecular weight.[47] The ratio $h = D_{linear}/D_{star}$ (contraction factor) compares the translational diffusion coefficients of the linear and star polymer of identical molecular weight. For a random walk chain, the value of h is calculated using eq 4:[47]

$$h = \frac{f^{1/2}}{2 - f + 2^{1/2}(f-1)} \quad (4)$$

where f is the number of arms, in this case $f = 4$, and $h = 0.897$. The 11.7k linear PNIPAM molecular weight lies between that of the 10k and 13k star polymers, and h will therefore be an estimate; comparing the ratios of the diffusion coefficients at 288 K provided $h = 0.868$ using the 10k star, and $h = 0.822$ using the 13k star. The value of h thus lies in the range 0.822−0.868 and is slightly lower than the random-walk value. Experimental values of h higher than the random-walk value indicate chain stretching due to steric crowding, common in stars of high functionality.[47] At the θ temperature (in this case defined as 1−2 degrees below the observed LCST), using the 13k star, $h = 0.91$ was obtained as expected because the hydrodynamic properties of branched and linear polymers become comparable with chain collapse.[48]

Figure 5 shows the log−log plot of the diffusion coefficient D (normalized for temperature and viscosity) versus molecular weight for a range of temperatures; the data demonstrates that the diffusion coefficient is mass dependent for star and linear chains over a range of temperatures. The slope provided by least-squares fits of the curves gives the critical exponent, υ_H.[49] In a good solvent, the exponent is expected to be close to 0.588.[47] The exponents obtained from the slopes of the plots in Figure 5 are listed in Table 3.

Under good solvent conditions (288 K), the exponents obtained from least-squares fits were −0.54 and −0.47 for the star and linear PNIPAM, respectively. A value of around −0.55 has been obtained experimentally for polymers in good solvents,[50] indicating that, in the case of the star PNIPAM at 288

Table 3. Values of the Flory Exponent, ν Obtained by Least-Square Fits of the Data in Figure 5 for Star and Linear PNIPAM at Various Temperatures

	ν_H 288 K	ν_H θ	ν_H LCST	ν_H 5 K > LCST
star	−0.54 ($R^2 = 0.9660$)	−0.47 ($R^2 = 0.9917$)	−0.42 ($R^2 = 0.9778$)	−0.10 ($R^2 = 0.9035$)
linear	−0.47 ($R^2 = 0.9973$)	−0.50 ($R^2 = 0.9976$)	−0.48 ($R^2 = 0.9964$)	−0.42 ($R^2 = 0.9789$)

K, water is a good solvent (the 10k star was not included in the plots because of its low LCST of 290 K). An exponent of −0.5 indicates a θ solvent,[47] so even at temperatures well below the LCST of the linear PNIPAM, water appears to be a poorer than θ solvent. The PNIPAM star data gives $D \sim M^{-0.47}$ at the θ temperature, and $D \sim M^{-0.42}$ at the LCST; an exponent of −0.33 represents a hard, dense sphere, so a dense collapsed chain is not formed. Above the LCST, the linearity is poor and the scaling relation breaks down. The linear PNIPAM showed $D \sim M^{-0.50}$ at the θ temperature as expected, and an exponent of −0.42 is obtained above the LCST. The decrease in the exponent in going from a good solvent (−0.47) to θ conditions (−0.50) may be due to the effects of partial draining;[47] expansion of a polymer chain in a good solvent lowers the chain density in the coil and may reduce the effective hydrodynamic size of the polymer in relation to the nondraining limit. The effects of partial draining are expected to reduce under θ conditions, and this may explain why the value of the exponent obtained under these conditions is as expected. This partial draining effect may affect linear and branched polymers to different degrees.[47]

The chain density in g/cm^3 of the star and linear PNIPAM was estimated using eq 5:[37]

$$\frac{M_W}{(4\pi/3\langle R_H\rangle^3 N_A)} \tag{5}$$

where M_W is weight-average molecular weight, R_H is the hydrodynamic radius, and N_A is Avogadro's constant.

Chain density was plotted as a function of temperature for star and linear PNIPAM (data not shown), and the sudden increase in the chain density around the LCST allowed a less ambiguous determination of the onset of chain collapse but correlated very well with the values obtained for a 50% reduction in integrated NMR peak area (Figures 2 and 3). A good correlation with dynamic light scattering measurements (discussed below) was also observed (for a comparison, see Table 6).

The chain densities calculated for the PNIPAM samples at different temperatures are shown in Table 4. The data illustrates that the chain densities for the 13k, 32k, and 52k stars are generally decreasing with increasing molecular weight, but the 10k star has a comparatively low chain density even above the LCST. The low chain density indicates that the smallest star cannot adopt a conformation as compact as the larger stars, and may reflect higher stretching of the chains that prevents close packing; the chain density of the 10k star mostly resembles the 11.7k linear chain across the entire temperature range. At 5 K above the LCST, the chain densities of the PNIPAM stars (with the exception of the 10k star) are much higher than the linear PNIPAM, so the star architecture permits the formation of a more compact globule; this is in line with theoretical predictions for star and linear polymers.[46] At a temperature 5 K above the θ temperature, the density of the stars increases with increasing molecular weight; a larger number of repeating units results in a denser globule. The trend for the linear PNIPAM is one of decreasing chain density with increasing molecular weight across the full range of temperatures.

Table 4. Comparison of Chain Densities for Star and Linear PNIPAM at Various Temperatures Across the LCST Transition

MW (NMR)	chain density 288 K (g/cm^3)	chain density at θ (g/cm^3)	chain density at LCST (g/cm^3)	chain density 5 K above LCST (g/cm^3)	total % increase in chain density[a]
			Star		
10 200	0.018	0.019	0.022	0.038	52.6
13 117	0.03	0.04	0.053	0.08	62.5
32 800	0.014	0.026	0.047	0.17	91.8
52 680	0.016	0.027	0.033	0.213	92.5
			Linear		
3 206	0.023	0.039	0.049	0.057	59.6
8 500	0.015	0.022	0.037	0.048	68.8
11 700	0.013	0.02	0.027	0.03	56.7

[a] Percentage change relative to the final density over the temperature range 288 to 5 K above the LCST.

The overall increases in chain density of the PNIPAM samples, expressed as a percentage of the final density, are also shown in Table 4. The star polymers show a higher overall increase in chain density with increasing molecular weight; there is no definite trend for the linear PNIPAM, but the overall increases are less than those for the parent star polymers. In the case of the linear PNIPAM, the chain densities do not increase significantly above the LCST, and the chains still contain a large amount of water. As a comparison, the 52k star has a chain density of 0.213 (79% water) at 5 K above the LCST; the corresponding linear PNIPAM of 11.7k molecular weight has a chain density of only 0.03 (97% water). A linear PNIPAM chain of molecular weight $>10^7$ was found to have a chain density of 0.2 g/cm^3 above the LCST.[19] The low molecular weight of the linear PNIPAM in this work must prevent the formation of a dense globule.

As a final comment, the overlap concentration, c^* (based on R_H) is equivalent to the chain density and ranges from 13 to 23 mg/mL for the PNIPAM samples at 288 K (Table 4). The value of c^* increases with increasing temperature, so the concentration of the PNIPAM samples studied in this work (1 and 10 mg/mL) are below c^*, and the solutions are therefore considered to be in the dilute regime.[46]

Decrease in R_H Below the LCST: The *n*-Cluster Model. The substantial decrease in R_H at temperatures below the LCST observed for star and linear PNIPAM in this work suggested that considerable change in the PNIPAM chain conformation occurs below the phase transition. Zhu and Napper[23,24] have invoked the "*n*-cluster" formation theory developed by de Gennes et al.[11] to explain similar observations from DLS studies of PNIPAM attached to the surfaces of polystyrene latex particles. They observed a coil-to-globule type transition below the LCST which manifested as a steady decrease in R_H, but the particles remained sterically stable until above the LCST, when flocculation occurred. Similar observations were made by Walldal et al.[51] for PNIPAM chains grafted to colloidal silica particles.

The "*n*-cluster" model describes the solution thermodynamics of a polymer−solvent mixture where the interaction of a monomer pair is repulsive (i.e., in a good solvent), but interactions between $n > 2$ monomers are attractive.[11,23,52,53] These *n*-clusters may indicate the formation of microaggregates or protomicelles, and are predicted for solutions of free chains as well as chains end-tethered to a surface.[52]

Zhu and Napper thus attributed the coil-to-globule behavior they observed under better than θ solvent conditions to *n*-cluster

Table 5. Calculated Values of *n*-Cclusters and Binary Cluster Contents for Star and Linear PNIPAM

MW (NMR)	ΔR_H (< θ)	ΔR_H (> θ)	% *n*-clusters	% binary
		Star		
10 200	0.15	0.92	18	82
13 117	0.39	1.01	22	78
32 800	0.89	1.85	32	68
52 680	0.9	2.28	28	72
		Linear		
3 206	0.30	0.19	61	39
8 500	0.34	0.56	36	64
11 700	0.42	1.39	23	77

formation, and the simultaneously occurring steric stabilization to repulsive binary interactions.[23,24] It has been predicted theoretically that *n*-cluster formation at interfaces can produce a vertical phase separation with an inner layer of globular, bulklike polymer chains and an outer layer that is more dilute.[11] This outer layer is responsible for the steric stabilization. This type of structuring is predicted to occur only when the temperature of the system is less than the θ temperature, which in the case of aqueous PNIPAM is 30.6 °C.[11,52,53]

Zhu and Napper calculated the change in R_H below and above the θ temperature (30.6 °C) and expressed the results as % *n*-cluster and % binary interactions. It should be noted that the polymers used in the work by Zhu and Napper were in the molecular weight range 3.2×10^5 to 2×10^6.[23] They found that, with decreasing molecular weight, the *n*-cluster contribution increased significantly. The relative balance between the two contributions was thus shown to be molecular weight dependent, but a clear explanation for the molecular weight dependence was not provided. A PFG-NMR study of an aqueous solution of linear PNIPAM of molecular weight 3.5×10^5 (3, 10, and 30 mg/mL in D_2O) was made by Larsson et al.;[14] only a slight change in diffusion properties, and hence R_H, was observed about 2 °C below the observed LCST of 32 °C, indicating only minor rearrangements of the chains occurred around the θ temperature. For a similar molecular weight PNIPAM, a tethered chain of molecular weight of 3.2×10^5 in the case of Zhu and Napper, and a free chain of molecular weight of 3.5×10^5 in the case of Larsson, it is apparent that tethering to a polystyrene latex affected the transition behavior, and substantial rearrangement of the chains occurred below the θ temperature.

To determine the contribution of *n*-clusters to the PNIPAM samples used in the present work, the decrease in R_H below and above the θ temperature was calculated for each of the polymers, and contributions of the two interactions were compared. Because the LCST of the star polymers was less than the θ-temperature of 30.6 °C and the LCST of the linear PNIPAM was higher than this temperature, the θ temperature in this case was defined as 1−2 degrees below the observed LCST (depending on the data available for a specific sample); the range over which changes in R_H were taken included the lowest measured temperature (288 K) to 5 degrees above the measured LCST. The changes in R_H below and above the θ temperature were defined as follows:

$$\Delta R_H (<\theta) = R_{H(288K)} - R_{H(\theta)} \quad (6)$$

$$\Delta R_H (>\theta) = R_{H(\theta)} - R_{H(LCST+5K)} \quad (7)$$

$$\% \; n\text{-clusters} = \Delta R_H (<\theta)/[\Delta R_H (<\theta) + \Delta R_H (>\theta)] \times 100 \quad (8)$$

$$\% \text{ binary} = 100 - \% \; n\text{-clusters} \quad (9)$$

The results for star and linear PNIPAM are listed in Table 5.

Table 6. LCST Values Obtained Using ^{1}H NMR, PFG-NMR, and DLS for Star and Linear PNIPAM; Particle Diameters Obtained Using PFG-NMR and DLS at 288 K

MW (NMR)	LCST 50% decrease in peak area	LCST chain density	DLS	diameter PFG-NMR (nm)	diameter DLS (nm)
		Star			
10 200	290−292	290	290	5.84	7.30
13 117	296	296	295	5.56	6.14
32 800	306	303	302	9.74	8.00
52 680	305	303	302	10.98	9.44
		Linear			
3 206	307−308	Not clear	307	3.66	3.48
8 500	307−308	308		5.64	
11 700	307−308	308		6.76	

The data shows that *n*-cluster contributions for the PNIPAM stars increase with increasing molecular weight from around 20% for the smaller stars to 30% for the larger stars. These observations are opposite to the molecular weight trend observed by Zhu and Napper, who found a decrease in *n*-cluster contributions with increasing molecular weight. In contrast, the *n*-cluster contributions for the linear PNIPAM decreased with increasing molecular weight in agreement with the trend described by Zhu and Napper for *tethered* PNIPAM. The decreasing levels of *n*-cluster contributions with increasing molecular weight observed for linear PNIPAM may be a reflection of chain flexibility. Chain flexibility increases with degree of polymerization, and this may influence the balance of binary and *n*-cluster contributions below the θ-temperature. In addition, the influence of the chain end in promoting *n*-cluster formation may be diminished at higher molar masses.

The *n*-cluster content calculated for the 8.5k and 11.7k linear PNIPAM and their corresponding parent stars are similar, suggesting that the tethered and free chains are being influenced in similar ways with increasing temperature. The 13k star and the corresponding 3k linear PNIPAM have *n*-cluster contents of 22% and 61%, respectively; the large difference in *n*-cluster content between the tethered and linear lower-molecular-weight chains must reflect the influence of the star core. As observed for the LCST transitions of the PNIPAM stars, the influence of the star core diminishes as the number of arm repeating units exceeds 70; the 32k and 52k stars have very similar *n*-cluster contributions.

The formation of *n*-clusters in the smaller stars may be inhibited by the hydrophobic nature of the star core and/or the tethering of the chains to the core. A hydrophobic environment promotes stronger polymer−polymer interactions, and thus a lower LCST, but why such an environment should inhibit the formation of *n*-clusters is unclear. It might be expected that the *n*-cluster contributions would *increase* with increasing hydrophobicity. The anchoring of the PNIPAM chains to the star core is expected to decrease chain flexibility, and this may inhibit *n*-cluster formation below the θ temperature. For tethered chains, the *n*-clusters are predicted to form nearer to the tethering point and to extend outward.[11] If the core region of the smaller stars is more expanded than that of the 32k and 52k stars, the lower percentage of *n*-clusters may be due to the stretching of the chains. As mentioned earlier, the expansion of the polymer chains in the core region can extend over most of the length of the polymer having small molecular weight and reduces in importance with increasing molecular weight.[27,45,46]

The *n*-cluster contents determined in this from PFG-NMR measurement do not correspond with the values of LCST measured of the particular polymers. The linear PNIPAM samples all have the same LCST, but widely different *n*-cluster

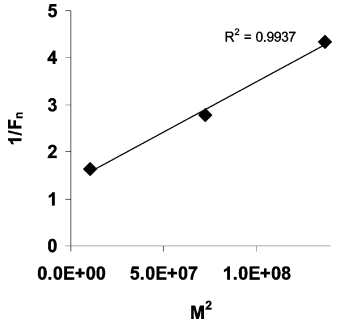

Figure 6. Reciprocal of the fraction of *n*-clusters formation ($1/F_n$) vs $M^{(n/2-1)}$ for linear PNIPAM, for $n = 6$.

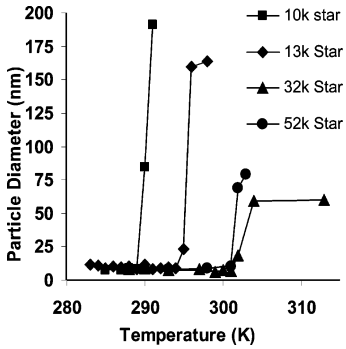

Figure 7. Particle diameter vs temperature for 10k, 13k, 32k, and 50k PNIPAM stars in D_2O obtained using DLS.

contributions. The 8.5k and 11.7k linear PNIPAM have similar *n*-cluster contributions to the 32k and 52k parent stars, but the LCST temperatures measured for the stars are 5 K lower than those obtained for the linear chains (see Table 6).

An estimate of the value of cluster size, *n*, i.e., the number of repeating units involved in an *n*-cluster, may be obtained by application of a scaling law. Zhu and Napper derived the following scaling relation for tethered PNIPAM chains.[23] They predicted that a plot of the reciprocal of the fraction of *n*-cluster formation (F_n) against $M^{(n/2-1)}$ should be linear. They tested values of *n* ranging from 3 to 6 and found the plot for $n = 3$ to be reasonably linear; plots of $n = 4$, 5, or 6 were decidedly nonlinear. They therefore suggested that the formation of *n*-clusters in tethered PNIPAM involved around three isopropyl groups. The same analysis was applied to the star and linear PNIPAM in this study. For the star polymers, this plot was nonlinear for all values of *n* ranging from 3 to 10 (6 is usually considered the upper limit). The linear PNIPAM data, however, was very linear ($R^2 = 0.99$) for $n = 6$ (see Figure 6). This suggests that *n*-cluster formation involves around six isopropyl groups for linear PNIPAM.

The failure to obtain linear plots with data for the star polymer is due to the contribution from the smaller stars because, as discussed above, the influence of the star core is molecular weight dependent. It would be useful to prepare larger PNIPAM stars with molecular weights of around 75 000 and 150 000 to determine whether *n*-cluster formation follows expected trends.

LCST Transition and Particle Size Analysis of Star and Linear PNIPAM Using Dynamic Light Scattering. Figure 7 shows the change in particle diameter with increasing temperature for the 10k, 13k, 32k, and 52k PNIPAM stars. The LCST is easily detected as a sudden increase in particle diameter. The size of aggregates formed above the LCST are largest for the smaller star polymers; if left for 20−30 min at temperatures above the LCST, all samples formed aggregates of size >1000 nm. The addition of a low concentration of sodium dodecyl sulfate (SDS, 93 mg/L <cmc)[23] prevented the formation of the large aggregates, but did not affect the location of the LCST. All samples contained low quantities of aggregated particles with diameters of 50−80 nm (1−5%) and ≈ 500 nm (0.1−0.5%), even at low temperatures, and with SDS added. The concentration of the aggregates increased up to 2-fold approaching the LCST and then dramatically at and above the transition. The proportion of aggregates formed was somewhat lower at 0.25 mg/mL than at 1 mg/mL, suggesting the interactions of particles to form aggregates is concentration dependent and occurs even at very low concentrations. The difference in the size of the aggregates formed from the lower molecular weight stars (160−200 nm) and the higher molecular weight stars (60−80 nm) above the LCST may reflect the reduced shielding of the hydrophobic star core by the low-molecular-weight PNIPAM chains. The 10k and 13k PNIPAM stars collapsed to form less dense particles than the higher-molecular-weight stars (see Table 4); this may allow stronger hydrophobic interactions between cores to occur and result in the formation of larger aggregates.

Table 6 compares the LCST values obtained for the star and linear PNIPAM using ^{1}H NMR, PFG-NMR, and DLS. The various methods of detecting the LCST provide similar results, although the values of LCST determined as the temperature of 50% decrease in NMR peak area tends to overestimate the values for some samples. The LCST values obtained using PFG-NMR and DLS are very close. Also, compared in Table 6 are the particle diameters obtained using PFG-NMR and DLS at 288 K. DLS appears to overestimate the size of the low-molecular-weight stars and to underestimate the size of the 32k and 52k stars. The 3k linear PNIPAM particle diameter obtained using DLS is close to the PFG-NMR result and confirms that the linear PNIPAM does not form micelles. It is necessary to mention that the decrease in particle diameter below the LCST observed using PFG-NMR could not be detected using DLS; all samples were measured in triplicate, but the variation within a group of measurements for a particular sample varied up to 25%. It may be that the particle size being measured is too small to accurately detect small size variations using DLS.

Conclusions

The LCST transitions and aqueous solution behavior of novel four-arm NIPAM star polymers and their hydrolyzed linear arms were studied using a combination of ^{1}H NMR, PFG-NMR, and DLS. Star polymer LCST transitions were found to be significantly lowered as a result of tethering of PNIPAM chains to the RAFT agent star core or to a combination of the core and benzyl end groups. The effect was molecular weight dependent and diminished once the number of repeating units per arm was ≥70. The liberated linear arms of the star polymers exhibited identical LCST transitions regardless of molecular weight and values higher than normally obtained for PNIPAM. The presence of a hydrophilic and hydrophobic end group on opposite ends of the polymer chain is suggested to cause this effect.

Diameters of the star and linear PNIPAM obtained from PFG-NMR and DLS measurements suggest the polymers adopt a relatively compact conformation even under good solvent conditions. The LCST transitions were broad, extending over a 10−15 °C range, and the low molecular weight of these chains may explain the observed transition broadening. The chain ends of the polymer arms carrying the RAFT agent benzyl end group showed decreased mobility with increasing temperature in all samples, indicating the chain ends interact with the PNIPAM. The compact size of the star and linear PNIPAM determined from PFG-NMR and DLS lead to this type of interaction.

The star polymers exhibited increasing chain density with increasing molecular weight above the LCST, while the opposite trend was observed for linear PNIPAM and indicates that the star polymers are able to collapse to form a denser globule as a result of the star architecture.

A significant decrease in R_H was observed below the LCST for star and linear PNIPAM using PFG-NMR and was attributed to the formation of *n*-clusters. The star polymers showed increasing *n*-cluster contributions with increasing molecular weight, while the linear PNIPAM showed the opposite trend. Successful application of a scaling law to the linear PNIPAM data indicated that the average size of the clusters was $n = 6$. Star polymer data did not obey a scaling law; the hydrophobic star core may inhibit *n*-cluster formation in the lowest-molecular-weight stars.

Particle diameters measured using DLS agreed reasonably well with PFG-NMR, and excellent agreement of LCST transitions between DLS and PFG-NMR was obtained. DLS experiments also revealed low concentrations of aggregates were present in the PNIPAM solutions below the LCST.

Acknowledgment. WE thank the Australian Research Council for funding of this project under LE0453637, LE0560981, and LE0668517. Financial assistance for R.P. from the University of Queensland and the Centre for Magnetic Resonance is also gratefully acknowledged.

References and Notes

(1) Schild, H. G. *Prog. Polym. Sci.* **1992**, *17*, 163−249.
(2) Nedelcheva, A. N.; Vladimirov, N. G.; Novakov, C. P.; Berlinova, I. V. *J. Polym. Sci., Part A: Polym. Chem.* **2004**, *42*, 5736−5744.
(3) Schilli, C. M.; Zhang, M.; Rizzardo, E.; Thang, S. H.; Chong, Y. K.; Edwards, K.; Karlsson, G.; Muller, A. H. E. *Macromolecules* **2004**, *37*, 7861−7866.
(4) Wang, Y.; Morawetz, H. *Macromolecules* **1989**, *22*, 164−167.
(5) Winnik, F. M.; Davidson, A. R.; Hamer, G. K.; Kitano, H. *Macromolecules* **1992**, *25*, 1876−1880.
(6) Zhu, M. Q.; Wang, L. Q.; Exarhos, G. J.; Li, A. D. Q. *J. Am. Chem. Soc.* **2004**, *126*, 2656−2657.
(7) Hales, M.; Barner-Kowollik, C.; Davis, T. P.; Stenzel, M. H. *Langmuir* **2004**, *20*, 10809−10817.
(8) Chung, J. E.; Yokoyama, M.; Aoyagi, T.; Sakurai, Y.; Okano, T. *J. Controlled Release* **1998**, *53*, 119−130.
(9) Schilli, C. M.; Muller, A. H. E.; Rizzardo, E.; Thang, S. H.; Chong, Y. K. *ACS Symp. Ser.* **2003**, *854*, 603−618.
(10) Zhulina, E. B.; Borisov, O. V.; Pryamitsyn, V. A.; Birshtein, T. M. *Macromolecules* **1991**, *24*, 140−149.
(11) Wagner, P.; Brochard-Wyart, F.; Hervert, H.; de Gennes, P. G. *Colloid Polym. Sci.* **1993**, *271*, 621−628.
(12) Afroze, F.; Nies, E.; Berghmans, H. *J. Mol. Struct.* **2000**, *554*, 55−68.
(13) Spevacek, J.; Hanykova, L.; Starovoytova, L. *Macromolecules* **2004**, *37*, 7710−7718.
(14) Larsson, A.; Kuckling, D.; Schonhoff, M. *Colloids Surf., A* **2001**, *190*, 185−192.
(15) Wu, C.; Zhou, S. *Macromolecules* **1995**, *28*, 8381−8387.
(16) Kujawa, P.; Segui, F.; Shaban, S.; Diab, C.; Okada, Y.; Tanaka, F.; Winnik, F. M. *Macromolecules* **2006**, *39*, 341−348.
(17) Winnik, F. M. *Macromolecules* **1990**, *23*, 1647−1649.
(18) Schild, H. G.; Tirrell, D. A. *J. Phys. Chem.* **1990**, *94*, 4352−4356.
(19) Wu, C. *Polymer* **1998**, *39*, 4609−4619.
(20) Fujishige, S.; Kubota, K.; Ando, I. *J. Phys. Chem.* **1989**, *93*, 3311−3313.
(21) Xia, Y.; Burke, A. D.; Stover, H. D. H. *Macromolecules* **2006**, 39, 2275−2283.
(22) Taylor, L. D.; Cerankowski, L. D. *J. Polym. Sci., Polym. Chem. Ed.* **1975**, *13*, 2551−2570.
(23) Zhu, P. W.; Napper, D. H. *Colloids Surf., A* **1996**, *113*, 145−153.
(24) Zhu, P. W.; Napper, D. H. *J. Colloid Interface Sci.* **1994**, *164*, 489−494.
(25) de Gennes, P. G. *Macromolecules* **1980**, *13*, 1069−1075.
(26) Yim, H.; Kent, M. S.; Mendez, S.; Balamurugan, S. S.; Balamurugan, S.; Lopez, G. P.; Satija, S. *Macromolecules* **2004**, *37*, 1994−1997.
(27) Dan, N.; Tirrell, M. *Macromolecules* **1992**, *25*, 2890−2895.
(28) Baulin, V. A.; Halperin, A. *Macromol. Theory Simul.* **2003**, *12*, 549−559.
(29) Baulin, V. A.; Halperin, A. *Macromolecules* **2002**, *35*, 6432−6438.
(30) Birshtein, T. M.; Zhulina, E. B. *Polymer* **1984**, *25*, 1453−1461.
(31) Mayadunne, R. T. A.; Jeffery, J.; Moad, G.; Rizzardo, E. *Macromolecules* **2003**, *36*, 1505−1513.
(32) Hasan, E.; Zhang, M.; Muller, A. H. E.; Tsvetanov, Ch. B. *J. Macromol. Sci., Part A: Pure Appl. Chem.* **2004**, *41*, 467−486.
(33) Johnson, C. S. *Prog. Nucl. Magn. Reson. Spectrosc.* **1999**, *34*, 203−256.
(34) Jerschow, A.; Muller, N. *J. Magn. Reson.* **1997**, *125*, 372−375.
(35) Stejskal, E. O.; Tanner, J. E. *J. Chem. Phys.* **1965**, *42*, 288−292.
(36) Zeng, F.; Tong, Z.; Feng, H. *Polymer* **1997**, *38*, 5539−5544.
(37) Wang, X., Qiu, X.; Wu, C. *Macromolecules* **1998**, *31*, 2972−2976.
(38) Sugiyama, K.; Sono, K. *J. Appl. Polym. Sci.* **2001**, *81*, 3056−3063.
(39) Menger, F. M.; Azov, V. A. *J. Am. Chem. Soc.* **2002**, *124*, 11159−11166.
(40) Postma, A.; Davis, T. P.; Moad, G.; O'Shea, M. S. *Macromolecules* **2005**, *38*, 5371−5374.
(41) Ding, Z.; Chen, G.; Hoffman, A. S. *Bioconjugate Chem.* **1996**, *7*, 121−125.
(42) Takei, Y. G.; Aoki, T.; Sanui, K.; Ogata, N.; Okano, T.; Sakurai, Y. *Bioconjugate Chem.* **1993**, *4*, 42−46.
(43) Birshtein, T. M.; Pryamitsyn, V. A. *Macromolecules* **1991**, *24*, 1554−1560.
(44) Ganazzoli, F.; Raos, G.; Allegra, G. *Macromol. Theory Simul.* **1999**, *8*, 65−84.
(45) Forni, A.; Ganazzoli, F.; Vacatello, M. *Macromolecules* **1997**, *30*, 4737−4743.
(46) Burchard, W. *Adv. Polym. Sci.* **1999**, *143*, 113−191.
(47) Roovers, J.; Zhou, L. L.; Toporowski, P. M.; van der Zwan, M.; Iatrou, H.; Hadjichristidis, N. *Macromolecules* **1993**, *26*, 4324−4331.
(48) Ganazzoli, F.; Forni, A. *Macromolecules* **1995**, *28*, 7950−7952.
(49) Forni, A.; Ganazzoli, F.; Vacatello, M. *Macromolecules* **1996**, *29*, 2994−2999.
(50) Batoulis, J.; Kremer, K. *Macromolecules* **1989**, *22*, 4277−4285.
(51) Walldal, C.; Wall, S. *Colloid Polym. Sci.* **2000**, *278*, 936−945.
(52) Sevick, E. M. *Macromolecules* **1998**, *31*, 3361−3367.
(53) Baulin, V. A. In *Physics*; Universite Joseph Fourier—Grenoble I: Grenoble, France, 1992.

MA0614545